

Stochastic energy-cascade model for 1+1 dimensional fully developed turbulence

Jürgen Schmiegl^a, Jochen Cleve^b, Hans C. Eggers^c,
Bruce R. Pearson^d, and Martin Greiner^e

^a*Network for Mathematical Physics and Stochastics, Aarhus University, DK-8000 Aarhus, Denmark; email: schmiegl@imf.au.dk*

^b*ICTP, Strada Costiera, 11, 34014 Trieste, Italy; email: cleve@ictp.trieste.it*

^c*Department of Physics, University of Stellenbosch, 7600 Stellenbosch, South Africa; email: eggers@physics.sun.ac.za*

^d*School of Mechanical Materials, Manufacturing Engineering and Management, University of Nottingham, Nottingham NG7 2RD, United Kingdom; email: bruce.pearson@nottingham.ac.uk*

^e*Corporate Technology, Information & Communications, Siemens AG, D-81730 München, Germany; email: martin.greiner@siemens.com*

Abstract

Geometrical random multiplicative cascade processes are often used to model positive-valued multifractal fields such as the energy dissipation in fully developed turbulence. We propose a dynamical generalization describing the energy dissipation in terms of a continuous and homogeneous stochastic field in one space and one time dimension. In the model, correlations originate in the overlap of the respective space-time histories of field amplitudes. The theoretical two- and three-point correlation functions are found to be in good agreement with their equal-time counterparts extracted from wind tunnel turbulent shear flow data.

Whenever strongly anomalous, intermittent fluctuations, long-range correlations, multi-scale structuring and selfsimilarity go hand in hand, the label ‘multifractality’ is attached to the underlying process. While in this Letter we have in mind fully developed turbulence of fluid mechanics [1], such processes occur in various other fields such as formation of cloud and rain fields in geophysics [2], internet traffic of communication network engineering [3], and stock returns in finance. [4], to name but a few.

Random multiplicative cascade models (RMCs) are commonly used to model and visualize such phenomena since they generally exhibit multifractality and reproduce the abovementioned properties [5]. They are usually implemented through a scale-independent cascade generator which produces a nested hierarchy of scales and multiplicatively redistributes the local measure.

In fully developed turbulence, RMCs have often been employed to model the energy flux through inertial-range scales. Due to their multiplicative nature, they can easily reproduce multifractal scaling exponents associated with the energy dissipation [6], the latter representing the intermittency corrections [1]. Although the link between such models and the Navier-Stokes equation remains unclear, recent investigations on multiplier distributions [7,8] and scale correlations [9] have shown that RMCs do appear to contain more truth than might reasonably be expected from their phenomenological basis.

Nevertheless, these discrete RMCs are purely geometrical constructs and incapable of describing causal dynamical effects of the turbulent energy cascade. A generalization in this direction is clearly desirable. Hence, in this Letter, we present a dynamical RCM in 1+1 space-time dimensions which respects causality and homogeneity. It is related to recent, related efforts [10,11,12,13], but goes beyond them in its dynamical interpretation. We first show how this model yields multifractal scaling for arbitrary n -point correlation functions, proceeding thereafter to compare equal-time two- and three-point correlation functions to their counterparts obtained from wind-tunnel turbulent shear flow data.

Our dynamical RCM is constructed by analogy to the geometrical case, in which the amplitude of the positive-valued energy-dissipation field, resolved at the dissipation scale η , is defined as the product of independently and identically distributed random weights $q(l_j)$,

$$\varepsilon(\eta) = \prod_{j=1}^J q(l_j) = \exp \left(\sum_{j=1}^J \ln q(l_j) \right), \quad (1)$$

where l_j is an element of a nested hierarchy of scales $\eta = l_J \leq l_j = L/\lambda^j \leq l_0 = L$ with $0 \leq j \leq J$ the ‘‘cascade generation’’ and $\lambda > 1$ the discrete scale step.

The integral length L and the dissipation length η represent, respectively, the largest and smallest length scale of the process. The geometrical RMCM furthermore requires $\langle q \rangle = 1$ because of conservation of energy flux.

We generalize (1) by assuming that ε is again the multiplicative product of a stochastic field, but that this field is now defined on continuous 1+1 spacetime:

$$\varepsilon(x, t) = \exp \left\{ \int_{-\infty}^{\infty} dt' \int_{-\infty}^{\infty} dx' f(x - x', t - t') \gamma(x', t') \right\}, \quad (2)$$

where f is the “index function” described below and by assumption $\gamma(x, t) \sim S_{\alpha}((dxdt)^{\alpha^{-1}-1}\sigma, -1, \mu)$ is a Lévy-stable white-noise field with index $0 \leq \alpha \leq 2$ [14]. For $\alpha=2$, this corresponds to a non-centered Gaussian white-noise field. From its characteristic function, $\langle \exp\{n\gamma\} \rangle = \exp\{-(\sigma^{\alpha}n^{\alpha})/(\cos(\pi\alpha/2)) + \mu n\}$ with $\alpha \neq 1$, the parameter μ is fixed to $\mu = \sigma^{\alpha}/\cos(\pi\alpha/2)$ in order to satisfy the requirement $\langle \exp\{\gamma\} \rangle = 1$.

Causality, i.e. the requirement that $\varepsilon(x, t)$ depends on the past but not the future, dictates that the index function $f(x - x', t - t')$ must be zero for $t - t' < 0$. Demanding also spatial symmetry around x , we are led to the form

$$f(x - x', t - t') = \begin{cases} 1 & (0 \leq t - t' \leq T, -g(t - t') \leq x - x' \leq g(t - t')) , \\ 0 & (\text{otherwise}) . \end{cases} \quad (3)$$

As illustrated in Fig. 1, the causality cone $g(t - t')$ incorporates a correlation time T and a correlation length L with $g(T) = L/2$. The exponent of the ansatz (2) can be thought of as a moving average over the stable white-noise field.

According to (3), the time integration in (2) runs over $0 \leq t - t' \leq T$. Since to any given time t_j there corresponds a length scale $l_j = 2g(t_j)$, there is a joint hierarchy of length and time scales, so that (2) factorizes into integrals of γ over the separate slices shown in Fig. 1,

$$q(l_j) = \exp \left\{ \int_{t-t_{j-1}}^{t-t_j} dt' \int_{x-g(t-t')}^{x+g(t-t')} dx' \gamma(x', t') \right\}. \quad (4)$$

In order to interpret $q(l_j)$ as a random multiplicative weight, its probability density needs to be independent of scale. Since the $\gamma(x', t')$ are i.i.d., the integration domain of (4) must therefore be independent of the scale index j . Together with the the boundary conditions $g(T - \Delta T_L) = L/2$ and $g(\Delta T_{\eta}) = \eta/2$,

this fixes the causality cone to

$$g(t-t') = \frac{(L/2)}{1 + \frac{(L-\eta)}{\eta} \frac{(T-\Delta T_L-(t-t'))}{(T-\Delta T_L-\Delta T_\eta)}} \quad (5)$$

for times $\Delta T_\eta \leq t-t' \leq T-\Delta T_L$. To complete the picture, we need to specify $g(t-t')$ for $0 \leq t-t' \leq \Delta T_\eta$ and $T-\Delta T_L \leq t-t' \leq T$. Since on physical grounds we expect $\Delta T_\eta \ll T$, the simplest choice is $\Delta T_\eta = 0$. For the remaining parameter ΔT_L , we assume $\Delta T_L \ll T$; it will be specified more fully below.

The construction proposed in Eqs. (2)-(5) guarantees that the one-point statistics of the dynamical RCM are identical to its geometrical counterpart. In order to qualify for a complete dynamical generalization, not only the one-point statistics but the n -point statistics in general should match. Hence, we now consider the equal-time two-point correlator with $t_1=t_2=t$ and $\Delta x = x_2-x_1 > 0$,

$$\begin{aligned} R_{n_1, n_2}(\Delta x) &= \frac{\langle \varepsilon^{n_1}(x_1, t) \varepsilon^{n_2}(x_2, t) \rangle}{\langle \varepsilon^{n_1}(x_1, t) \rangle \langle \varepsilon^{n_2}(x_2, t) \rangle} \\ &= \frac{\langle D(\Delta x)^{n_1+n_2} \rangle}{\langle D(\Delta x)^{n_1} \rangle \langle D(\Delta x)^{n_2} \rangle}. \end{aligned} \quad (6)$$

As shown in Fig. 2a, the correlation between two points a distance $\eta \leq \Delta x \leq L$ apart stems from the overlap region of the two index functions $f(x'-x_1, t)$ and $f(x_2-x', t)$. This explains why, in the second step of (6), R can be written solely in terms of integrals D over the overlap region,

$$D(\Delta x) = \exp \left(\int_{t-T}^{t-g^{(-1)}(\Delta x/2)} dt' \int_{x_2-g(t-t')}^{x_1+g(t-t')} dx' \gamma(x', t') \right), \quad (7)$$

since the contributions from the non-overlapping regions are statistically independent and hence factorize and cancel. Introducing the spatio-temporal overlap volume

$$\begin{aligned} V(\Delta x) &= \int_{t-T}^{t-g^{(-1)}(\Delta x/2)} dt' \int_{x_2-g(t-t')}^{x_1+g(t-t')} dx' \\ &= \frac{\eta L(T-\Delta T_\eta)}{(L-\eta)} \ln \left(\frac{L}{\Delta x} \right) - \left(\frac{\eta(T-\Delta T_\eta)}{(L-\eta)} - \Delta T_L \right) (L-\Delta x), \end{aligned} \quad (8)$$

and employing basic properties of stable distributions [14], the expectation of

the n -th power of D is found to be

$$\langle D(\Delta x)^n \rangle = \exp \left(\frac{\sigma^\alpha}{\cos \frac{\pi\alpha}{2}} V(\Delta x)(n - n^\alpha) \right). \quad (9)$$

Defining the multifractal scaling exponents $\tau(n) = \tau(2)(n - n^\alpha)/(2 - 2^\alpha)$, with $\tau(2) = (\sigma^\alpha / \cos \frac{\pi\alpha}{2})(2 - 2^\alpha)\eta L(T - \Delta T_\eta)/(L - \eta)$, as well as $\tau[n_1, n_2] = \tau(n_1 + n_2) - \tau(n_1) - \tau(n_2)$, substitution of (9) into (6) leads to the final expression for the equal-time two-point correlator:

$$\begin{aligned} R_{n_1, n_2}(\Delta x) &= \\ &= \left(\frac{L}{\Delta x} \right)^{\tau[n_1, n_2]} \exp \left[-\tau[n_1, n_2] \left(1 - \frac{(L - \eta)\Delta T_L}{\eta(T - \Delta T_\eta)} \right) \left(1 - \frac{\Delta x}{L} \right) \right]. \end{aligned} \quad (10)$$

Equal-time two-point statistics of our dynamical RMCM in 1+1 dimensions hence show multiscaling behavior for $\eta < \Delta x \ll L$, in complete analogy to the findings of the corresponding geometrical RMCM [15]. We also note that setting $\Delta T_L = (T - \Delta T_\eta)\eta/(L - \eta)$ eliminates the second factor in (10) leaving $R_{n_1, n_2}(\Delta x) = (L/\Delta x)^{\tau[n_1, n_2]}$ to scale rigorously.

Turning to temporal two-point correlations, we follow the same recipe as for the above. Correlations in this case arise from the overlap volume illustrated in Fig. 2b, and lead, after an analogous straightforward calculation, to

$$\begin{aligned} R_{n_1, n_2}(\Delta t) &= \frac{\langle \varepsilon^{n_1}(x, t_1) \varepsilon^{n_2}(x, t_2) \rangle}{\langle \varepsilon^{n_1}(x, t_1) \rangle \langle \varepsilon^{n_2}(x, t_2) \rangle} \\ &= \left(\frac{\Delta t - \Delta T_L}{T - \Delta T_L} + \frac{\eta}{L} \left(1 - \frac{\Delta t - \Delta T_L}{T - \Delta T_L} \right) \right)^{-\tau[n_1, n_2](1 - \Delta T_L/T)} \\ &\approx \left(\frac{T}{\Delta t} \right)^{\tau[n_1, n_2]} \end{aligned} \quad (11)$$

with $\Delta t = t_2 - t_1$ and $x_1 = x_2 = x$. For simplicity, the parameter ΔT_η has been set to zero. The last step of (11), valid for $\Delta T_L \ll \Delta t < T$ and $\eta \ll L$ only, shows that the temporal two-point correlator has scaling exponents identical to those of the equal-time counterpart.

Although respective spatio-temporal overlap volumes are more complicated, two-point spacetime correlations with both $\Delta x \neq 0$ and $\Delta t \neq 0$ can also be derived; see Ref. [16] for a complete analysis. Here, we prefer to continue with equal-time three-point correlations; their generalization to equal-time n -point correlations is straightforward and explicit expressions can again be found in Ref. [16]. The corresponding overlap volumes, illustrated in Fig. 2c, represent the starting point for a calculation analogous to (7)-(9), which leads to

$$\begin{aligned}
R_{n_1, n_2, n_3}(x_1, x_2, x_3) &= \frac{\langle \varepsilon^{n_1}(x_1, t) \varepsilon^{n_2}(x_2, t) \varepsilon^{n_3}(x_3, t) \rangle}{\langle \varepsilon^{n_1}(x_1, t) \rangle \langle \varepsilon^{n_2}(x_2, t) \rangle \langle \varepsilon^{n_3}(x_3, t) \rangle} \\
&= \left(\frac{L}{x_3 - x_1} \right)^{\tau[n_1 + n_2, n_3] - \tau[n_2, n_3]} \left(\frac{L}{x_2 - x_1} \right)^{\tau[n_1, n_2]} \left(\frac{L}{x_3 - x_2} \right)^{\tau[n_2, n_3]} \\
&\quad \exp \left\{ - \left(1 - \frac{(L - \eta) \Delta T_L}{\eta(T - \Delta T_\eta)} \right) \left[(\tau[n_1 + n_2, n_3] - \tau[n_2, n_3]) \left(1 - \frac{x_3 - x_1}{L} \right) \right. \right. \\
&\quad \left. \left. + \tau[n_1, n_2] \left(1 - \frac{x_2 - x_1}{L} \right) + \tau[n_2, n_3] \left(1 - \frac{x_3 - x_2}{L} \right) \right] \right\} \quad (12)
\end{aligned}$$

with $x_1 < x_2 < x_3$ and $\eta \leq x_i - x_j \leq L$ for all $i > j = 1, 2, 3$. In the case of $n_1 = n_2 = n_3 = 1$ and small separations $|x_i - x_j| \ll L$, or for all separations if the parameter ΔT_L is fine-tuned, this simplifies to

$$\begin{aligned}
R_{1,1,1}(x_2 - x_1 = \text{const}, x_3 = x) & \\
\sim \begin{cases} \left(\frac{L}{x - x_1} \right)^{\tau(2)} \left(\frac{L}{x_2 - x} \right)^{\tau(2)} & (x_1 < x < x_2) \\ \left(\frac{L}{x - x_1} \right)^{\tau(3) - 2\tau(2)} \left(\frac{L}{x - x_2} \right)^{\tau(2)} & (x_1 < x_2 < x) \end{cases} \quad (13)
\end{aligned}$$

The comparative ease with which the three-point expressions (12) and (13) were derived can be traced back to the fact that the present model incorporates spatio-temporal homogeneity from the very beginning. This is to be contrasted with the geometrical RMCs of (1) which, due to their hierarchical structure, are not translationally invariant in space. This non-invariance feeds through to all n -point observables and has to be removed at considerable cost through successive spatial sampling [17] before the latter can be compared to experimental counterparts.

While we expect the model proposed in this Letter to find application in many different phenomena, we demonstrate its qualities through comparison with fully developed turbulence data. A velocity record of the longitudinal component, obtained in a wind-tunnel shear flow experiment [18], was transformed into a one-dimensional spatial record of the positive-valued surrogate energy dissipation $\varepsilon(x) = 15\nu(\partial_x v_x)^2$, where ν is the viscosity. The sampled two-point correlations of order $n_1 = n_2 = 1$ and $n_1 = 2, n_2 = 1$ are plotted in Fig. 3. Within the inertial range $\eta \ll |x_2 - x_1| \ll L$, the data reveals rigorous power-law scaling with exponents $\tau[1, 1] = 0.184$ and $\tau[2, 1] = 0.34$. This fixes the intermittency exponent $\tau(2) = 0.184$ and the stable index $\alpha = 1.80$, which are the relevant model parameters for multifractal scaling. Once these have been fixed, no further room for adjustment is left for the theoretical three-point correlation (13), which is compared to its experimental counterpart in Fig. 4. Independent of the various combinations for the two-point distances $\eta \ll |x_i - x_j| \ll L$, the agreement between model and data is remarkable. This demonstrates that the proposed stochastic process, whose parameters

have been fixed from lowest-order two-point correlations, is capable to describe the equal-time multivariate statistics of the turbulent energy dissipation beyond two-point order. It proves also that the turbulent energy cascade can be thought of as a consistent multifractal process.

The dynamical RCMCM presented here is a generalization of the geometrical RCMCM. By construction, it is causal, continuous and homogeneous, does not make use of a discrete hierarchy of scales and stochastically evolves a positive-valued field in one space and one time dimension. Several generalizations of this new model come to mind immediately, such as the stochastic evolution in $n+1$ dimensions with the optional inclusion of spatial anisotropy, the use of independently scattered random measures to describe deviation from log-stability [19], the discretisation of space-time into smallest cells to model dissipation, and a dynamical RCMCM for vector fields to model the turbulent velocity field.

References

- [1] U. Frisch, *Turbulence*, (Cambridge University Press, Cambridge, 1995).
- [2] D. Schertzer and S. Lovejoy, J. Geophys. Res. **92** (1987) 9693.
- [3] K. Park and W. Willinger (eds), *Self-similar network traffic and performance evaluation*, John Wiley & Sons, New York, (2000).
- [4] J. Muzy, J. Delour and E. Bacry, Eur. Phys. J. B **17** (2000) 537.
- [5] J. Feder, *Fractals*, Plenum Press, New York, (1988).
- [6] C. Meneveau and K. Sreenivasan, J. Fluid Mech. **224** (1991) 429.
- [7] B. Jouault, P. Lipa and M. Greiner, Phys. Rev. E **59** (1999) 2451.
- [8] B. Jouault, M. Greiner and P. Lipa, Physica D **136** (2000) 125.
- [9] J. Cleve and M. Greiner, Phys. Lett. A **273** (2000) 104.
- [10] F.G. Schmitt and D. Marsan, Eur. Phys. J. B **20** (2001) 3.
- [11] J. Barral and B. Mandelbrot, Prob. Theory Relat. Fields **124** (2002) 409.
- [12] J.F. Muzy and E. Bacry, Phys. Rev. E **66** (2002) 056121.
- [13] F.G. Schmitt, arXiv:cond-mat/0305655.
- [14] G. Samorodnitsky and M. Taqqu, *Stable non-Gaussian random processes*, Chapman & Hall, New York, (1994).
- [15] J. Cleve, K.R. Sreenivasan and M. Greiner, in preparation.

- [16] J. Schmiegel, *Ein dynamischer Prozess für die statistische Beschreibung der Energiedissipation in der vollentwickelten Turbulenz*, PhD Thesis, TU Dresden, (2002).
- [17] H.C. Eggers, T. Dziekan and M. Greiner, Phys. Lett. A **281** (2001) 249.
- [18] B.R. Pearson, P.A. Krogstad and W. van de Water, Phys. Fluids **14** (2002) 1288.
- [19] O.E. Barndorff-Nielsen and J. Schmiegel, MAPHYSTO Research Report 2003-20 (<http://www.maphysto.dk>).

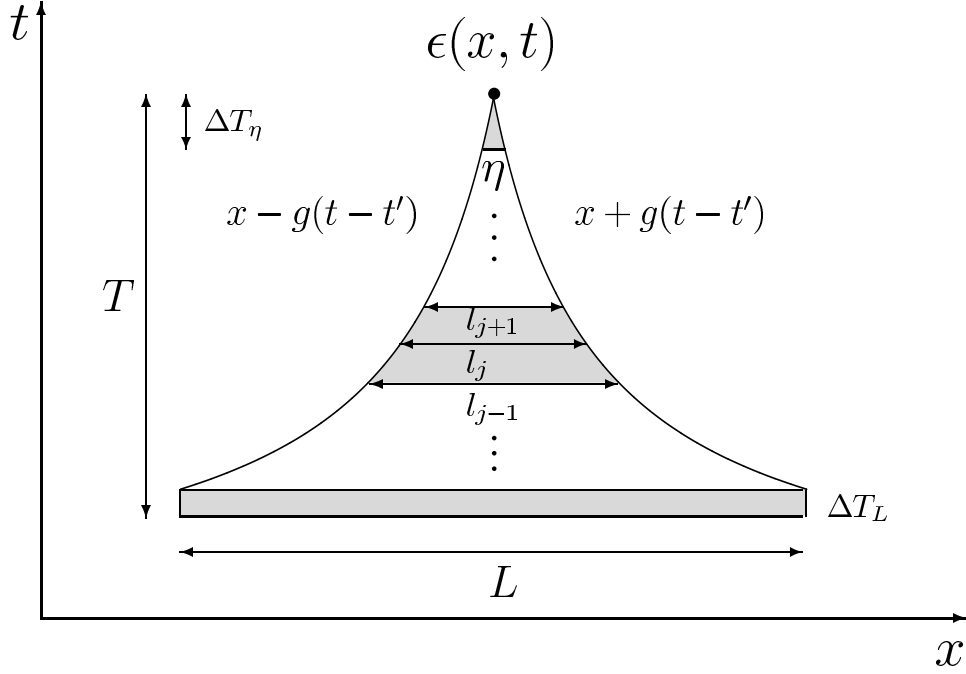


Fig. 1. Causal space-time “cone” for the positive-valued multifractal field $\varepsilon(x, t)$. All field amplitudes $\gamma(x', t')$ inside the causal space-time “cone” bordered by the index function (3) contribute multiplicatively to ε . See text for further detail.

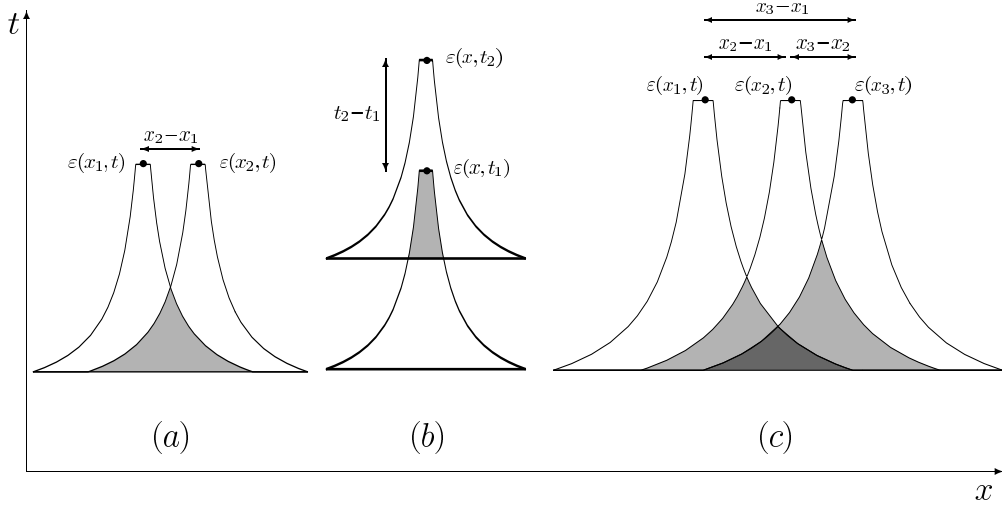


Fig. 2. Spatio-temporal overlap volumes (shaded) producing the correlation for the (a) equal-time and (b) temporal two-point correlator, as well as (c) for the equal-time three-point correlator. To simplify visualization, parameters have been set to $\Delta T_\eta = \Delta T_L = 0$.

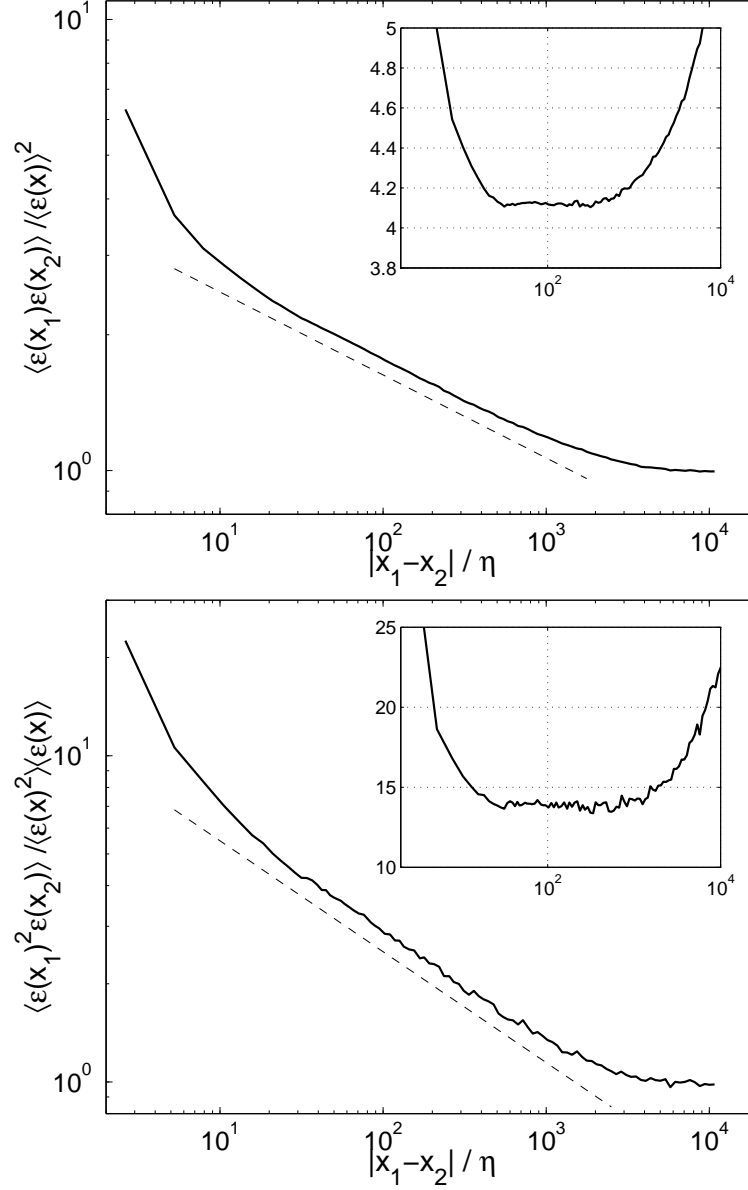


Fig. 3. Two-point correlator $\langle \varepsilon^{n_1}(x_1, t) \varepsilon^{n_2}(x_2, t) \rangle / (\langle \varepsilon^{n_1}(x_1, t) \rangle \langle \varepsilon^{n_2}(x_2, t) \rangle)$ of orders (a) $n_1 = n_2 = 1$ and (b) $n_1 = 2, n_2 = 1$ for the experimental shear-flow dataset [18] with Taylor Reynolds number $R_\lambda = 860$ and integral length scale $L = 1960\eta$ as a function of the distance $|x_2 - x_1|$ in units of the dissipation length η . The insets represent the compensated plots, where the two-point correlators have been divided by $(|x_2 - x_1| / \eta)^{-\tau[n_1, n_2]}$ with $\tau[1, 1] = 0.184$ and $\tau[2, 1] = 0.34$, respectively.

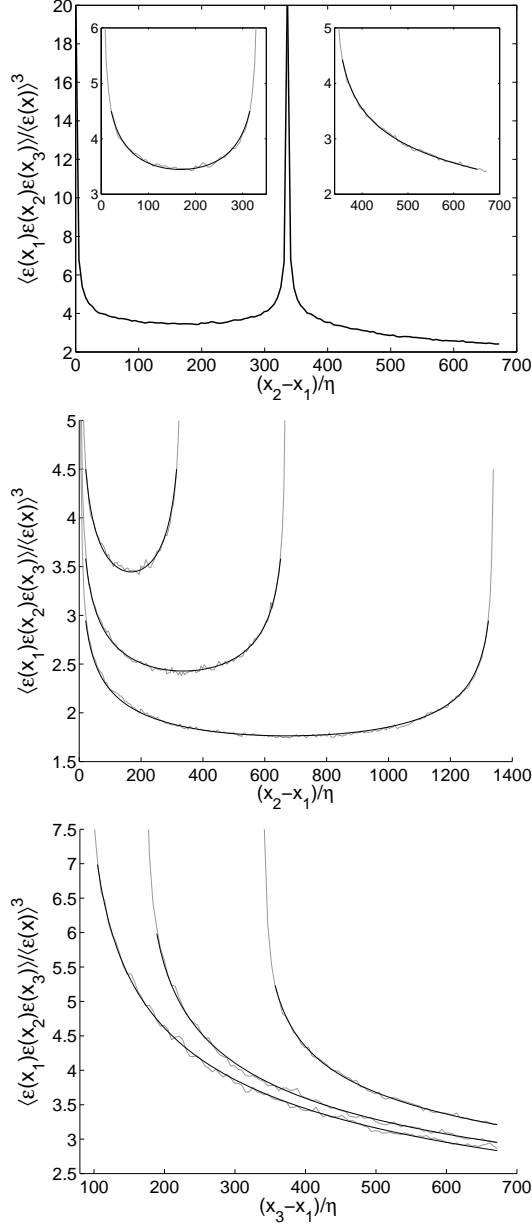


Fig. 4. Comparison between expression (13) and the experimentally extracted three-point correlator $\langle \varepsilon(x_1, t)\varepsilon(x_2, t)\varepsilon(x_3, t) \rangle / \langle \varepsilon(x, t) \rangle^3$. The same data set as in Fig. 3 has been used. The scaling exponents $\tau[1, 1] = 0.184$ and $\tau[2, 1] = 0.34$ have already been fixed by the two-point correlators. In part (a), the experimental three-point correlator is shown for a fixed two-point distance $x_2 - x_1 = 336\eta$. The two insets represent the comparison with (13) for the two regimes $\eta < x_3 - x_1 < x_2 - x_1$ and $x_3 - x_1 > x_2 - x_1$. Part (b) focuses on the regime $\eta < x_2 - x_1 < x_3 - x_1$ with fixed $(x_3 - x_1)/\eta = 336, 672$ and 1344 , respectively, while (c) focuses on the regime $x_3 - x_1 > x_2 - x_1$ with fixed $(x_2 - x_1)/\eta = 84, 168$ and 336 , respectively. For clarity, from left to right the curves of (c) have been shifted by 0, 0.4 and 0.8 along the y-axis.